Mitogen Inducible Gene-6 Is a Prognostic Marker for Patients with Colorectal Liver Metastases[1,2]

David B. Donner[*,†,3], Dan T. Ruan[*,†,3], Kan Toriguchi[*,†], Emily K. Bergsland[†,‡], Eric K. Nakakura[*,†], Meng Hsun Lin[*,†], Ricardo J. Antonia[*,†] and Robert S. Warren[*,†]

[*]Department of Surgery, Division of Surgical Oncology, and The Comprehensive Cancer Center, The University of California San Francisco, San Francisco, CA. 94143; [†]The Helen Diller Family Comprehensive Cancer Center, The University of California San Francisco, San Francisco, CA. 94143; [‡]Department of Medicine, Division of Hematology/Oncology, The University of California San Francisco, San Francisco, CA. 94143

Abstract

PURPOSE: Prognostic schemes that rely on clinical variables to predict outcome after resection of colorectal metastases remain imperfect. We hypothesized that molecular markers can improve the accuracy of prognostic schemes. METHODS: We screened the transcriptome of matched colorectal liver metastases (CRCLM) and primary tumors from 42 patients with unresected CRCLM to identify differentially expressed genes. Among the differentially expressed genes identified, we looked for associations between expression and time to disease progression or overall survival. To validate such associations, mRNA levels of the candidate genes were assayed by qRT-PCR from CRCLM in 56 additional patients who underwent hepatectomy. RESULTS: Seven candidate genes were selected for validation based on their differential expression between metastases and primary tumors and a correlation between expression and surgical outcome: lumican; tissue inhibitor metalloproteinase 1; basic helix-loop-helix domain containing class B2; fibronectin; transmembrane 4 superfamily member 1; mitogen inducible gene 6 (*MIG-6*); and serpine 2. In the hepatectomy group, only *MIG-6* expression was predictive of poor survival after hepatectomy. Quantitative PCR of *MIG-6* mRNA was performed on 25 additional hepatectomy patients to determine if *MIG-6* expression could substratify patients beyond the clinical risk score. Patients within defined clinical risk score categories were effectively substratified into distinct groups by relative *MIG-6* expression. CONCLUSIONS: *MIG-6* expression is inversely associated with survival after hepatectomy and may be used to improve traditional prognostic schemes that rely on clinicopathologic data such as the Clinical Risk Score.

Translational Oncology (2019) 12, 550–560

Introduction

Hepatic resection combined with chemotherapy is the standard treatment for patients with hepatic colorectal cancer metastases (CRCLM) and can lead to a 5-year survival of 30% to 58% [1,2]. The improved survival compared to chemotherapy alone, where patients rarely survive beyond 5 years, is ascribed to improvements in operative techniques, perioperative management, better imaging, and more effective chemotherapy. Two first-line therapies, 5-fluorouracil-leucovorin-oxaliplatin and 5-fluorouracil-leucovorin-irinotecan, are approved for advanced-stage CRCLM [3,4]. However, substantial

heterogeneity remains in outcomes for patients undergoing resection of CRCLM.

As surgeons become increasingly aggressive in resecting CRCLM, frequently accepting patients over 80 years old and with more extensive comorbidities, it becomes increasingly important to use prudent patient selection criteria based on biologic determinants of outcome. Thus, scoring systems have been developed with the goal of stratifying patients considered for liver resection into risk groups. Such prognostic schemes utilize clinicopathologic variables to estimate the risk of recurrence and death after hepatectomy for CRCLM [5–9]. Patients with a low risk of recurrence after hepatectomy may not benefit from neoadjuvant or adjuvant chemotherapy and may avoid the toxicity of perioperative chemotherapy [10]. However, when the risk of recurrence is high or the chance of complete resection is in question, delayed hepatectomy after a period of neoadjuvant therapy should be considered [11]. A neoadjuvant treatment course provides time to determine whether additional disease is present, allows assessment of tumor response to chemotherapy, and may facilitate complete tumor resection in patients with extensive hepatic metastases [12]. The potential benefits of delayed resection should be weighed against the risk of preoperative hepatotoxicity, disease progression, and the higher complication rates associated with hepatectomy after neoadjuvant therapies [13]. Although no clinical feature should absolutely exclude a patient from potentially curative hepatectomy, nonoperative management should be considered in those with an exceedingly high risk of recurrence and poor performance status.

The Clinical Risk Score (CRS) is a prognostic scheme composed of five preoperative variables: tumor number; largest tumor diameter; lymph node status during resection of the primary tumor; disease-free interval; and serum carcinoembryonic antigen level [5]. These are factors prognostic for clinical outcome and are generally available in the preoperative evaluation of patients. The CRS ranges from 0 to 5, depending on the number of unfavorable characteristics present. Each variable in the CRS is equally weighted with a single point for each unfavorable characteristic. Ideal candidates for hepatectomy have solitary metastases with a diameter less than 5 cm, serum CEA (carcinoembryonic antigen) <200 ng/ml, metachronous disease, and negative regional lymph nodes found at resection of the primary tumor (i.e., CRS = 0). However, even the most favorable CRS of 0 is associated with a 5-year actuarial survival rate of only 60%. Thus, patients within the lowest CRS category are still at risk of recurrence and death.

Although the CRS is a validated prognostic system, it remains imperfect [14]. One investigation of long-term outcomes after hepatectomy found that patients with a CRS of 0-2 had a 10-year actuarial survival rate twice as high as patients with a CRS of 3-5 (21% versus 10%) [15]. However, no preoperative clinical feature or CRS precluded a curative outcome in that study. One other study that attempted external validation of three prognostic schemes for CRCLM, including the CRS, failed to confirm any predictive utility in a cohort of 662 patients [16]. Recently, Dupre et al. reported that scoring systems by themselves are of limited value for stratifying patients operated on for recurrent colorectal liver metastases [17]. We have sought to improve prognostic schemes in order to better guide clinicians in the application of individualized treatment plans and to determine the best therapeutic course for their patients.

The molecular heterogeneity of colorectal cancer leads to large variations in the response of individual patients to therapy [18].

Microsatellite instability and a small group of molecular markers, including the mutational status of the *BRAF* and *KRAS* genes, are used for treatment decisions and patient stratification. However, groups of patients defined by these molecular markers still differ significantly in their responses to therapy. In recent years, several approaches to further subtype CRC have come into use, and among the most powerful of these is gene expression profiling, which can improve on the limitations of single gene testing. Gene expression profiling has defined subtypes of colorectal cancers that are predictive or prognostic of patient responses to therapies. [18]

In the present study, we sought to find prognostic markers for CRCLM and to determine if such markers could improve the accuracy of the CRS. We used microarrays to compare the transcriptome in CRCLM versus their primary tumors. From a group of genes with differential expression between CRCLM and their primary tumors, we selected a subgroup of genes with expression levels that associated with survival or time to disease progression. We validated the findings by quantitative PCR of mRNA from additional patients and found one gene, mitogen inducible factor-6 (*MIG-6*), which was predictive of poor survival. Lastly, we tested whether *MIG-6* expression could substratify patients within defined CRS categories. Our results show that molecular subtypes can complement clinical risk stratification to distinguish lower- from higher-risk patients with CRCLM.

Materials and Methods

Tumor Retrieval and RNA Extraction

All institutional review board requirements for human studies were met, and informed consent was obtained from all patients. All tissues were obtained at the time of surgery. All tissues were obtained at the time of surgery. Resected or Tru-cut needle biopsied (superficial) liver metastases (0.5-1.0 g) were snap frozen in the operating room within 2 minutes of harvest by transfer to a Dewar flask containing liquid nitrogen, transported to the laboratory, and stored at –80°C. Similarly, samples of resected primary colon or rectal tumors were taken in the operating room under the observation of a pathologist to preserve surgical and pathological margins and then snap frozen.

Matched samples of primary colon tumor (T); normal colon (N); and, in all but 6 cases, metastatic tumors of the liver (M) were obtained from each of 42 patients treated at the University of California at San Francisco Medical Center. Laser capture microdissection was performed on frozen tissue sections to separate normal and cancerous epithelial cells from surrounding stromal elements.

RNA Extraction

RNA was extracted from tissue lysates using the RNeasy kit (Qiagen, Inc., Valencia, CA) and amplified using an *in vitro* transcription-mediated procedure that maintains relative abundances of mRNAs [19]. Each sample was separately labeled with Cy3 and Cy5 fluorescent dyes. Prior to labeling, nonhuman RNA transcripts corresponding to control clones on microarrays were spiked into each sample in known amounts. The amounts of the spiked control transcripts were varied between the Cy3- and Cy5-labelings to create known differentials in the levels of some of these genes. Cy3- or Cy5-labeled nucleotides were incorporated during first-strand cDNA synthesis by reverse transcription using SuperScript II (Invitrogen Corp., Carlsbad, CA), primed with $(dT)_{25}$ and random nonamers

(Amersham Biosciences Corp., Piscataway, NJ). Following RNase digestion, the labeled probe was purified using the QIAquick PCR purification kit (Qiagen, Inc., Valencia, CA).

cDNA Microarray Assays

DNA microarray analysis was performed as described [20]. mRNA expression was measured using two-color microarrays containing different sets of cDNA clones. The dsDNA clones were produced by PCR using primers complementary to the vector sequences flanking the cDNA inserts. Each slide included approximately 384 human "housekeeping" genes and non-human (e.g. Arabidopsis thaliana, Drosophila melanogaster, plasmid, etc.) clones for quality control. PCR products were assessed for purity and yield by agarose-gel electrophoresis and were sequenced to verify their identities. Clones found to contain Alu repetitive elements were excluded from further analysis. A total of 36,518 clones that passed the quality criteria were assigned to 1 of 17,708 unique transcripts by GenBank accession number, representing 10,671 unique genes by LocusLink ID. Of these, 6501 genes were measured by at least 2 clones, usually with different sequences. After hybridization and washing, slides were scanned with a Generation III scanner (Molecular Dynamics). Relative gene expression was measured between pairs of co-hybridized samples. Depending on what samples were available from each patient, three comparisons of expression levels were made: metastatic tumor vs. primary tumor (M/T), primary tumor vs. normal epithelium (T/N), and metastatic tumor vs. normal epithelium (M/N). In each comparison, the pair of samples was measured twice with reverse labeling to eliminate bias introduced by the fluorescence properties of the different dyes. For 32 of the patients, T/N, M/N and M/T expression were all measured.

Microarray Data Analysis

Microarray image analysis was performed using ImaGene software (BioDiscovery, El Segundo, CA). For each spot, the median pixel intensity and standard deviation were determined, as well as the spot area, signal area, and local background intensity. For each cDNA clone, the results from four spots (two duplicates per slide, Cy3 and Cy5 labeled) were averaged, and a standard deviation was calculated. A clone was detected if its signal was at least 5 standard deviations above background. A ratio of expression between the two samples and its uncertainty were calculated from the intensities. Each array was normalized such that the median ratio observed among the clones measuring genes spiked into the Cy3 and Cy5 samples in equal amounts was one. A global normalization was then applied such that the median ratio observed across all of the cDNA spots on all of the arrays for each sample was 1. For each ratio, a significance call was assigned: undetected (in both the numerator and denominator), on (detected in the numerator only), off (detected in the denominator only), up or down (significantly over-expressed in the numerator or denominator, respectively), or equal (detected, but ratio not significantly different from one). To be called significantly up- (down-) regulated, a gene's expression must not only be greater (less) than the cut, but it had to be greater (less) than 1 with at least 95% certainty based on the uncertainty in the log ratio.

For the 32 patients that had T/N, M/N, and M/T expression measurements, consistency was required between the results of the three measurements for each spot, such that $4/5 < (T/N)*(M/T)/(M/N) < 5/4$, i.e., the three ratios should cancel to give a value of 1 within 25%. A list of genes that were differently expressed by more than 1.5-fold between the metastatic and primary tumors of these patients was generated. The number of ratios deemed sufficiently well measured to use (detected; consistent between T/N, M/N, and M/T measurements) varied for different spots. At least 10 good measurements were required for each spot to be considered. A total of 22,344 of 36,518 spots, assigned to 8027 of the 10,671 unique genes on the arrays, passed this criterion. Maximum likelihood estimates of the upper and lower 99% confidence limits on the prevalence in the parent population were calculated for each spot on the basis of the number of ratios exceeding the cut out of the number of good ratios. Spots judged to be up- or downregulated in 20% of the parent population with 99% certainty were included in the list. Thus, if only 10 good ratios were measured for a particular spot, 7 would have to make the cut (70%); if there were 32 good ratios, 14 would suffice (43%). When more than one spot assigned to a particular gene met these criteria, their average expression ratio in each patient was calculated, weighted by the inverse uncertainty squared for each ratio.

RT and qRT-PCR

cDNAs were synthesized from 2 μg total RNA using a SuperScript III first-strand synthesis kit. One microliter of the first cDNA synthesis mix was dispensed in triplicate and mixed with Taqman Universal PCR Mastermix and Taqman Gene Expression Assays in an end-volume of 10 μl into optical 384-well plates for Taqman RT-PCR. PCR primers for *MIG-6* [Hs00219060_m1], fibronectin 1 (HS00415006_m1), tissue inhibitor of metalloproteinase-1 [Hs00171558_m1], serine proteinase inhibitor member 2 [Hs00299953_m1], lumican [Hs00158940_m1], basic helix-loop-helix domain containing class B2 [Hs00186419], transmembrane 4 superfamily member-1 [Hs00371997], and the TaqMan probe were obtained from Applied Biosystems. Actin-B [Hs99999903_m1] was chosen as an endogenous normalization control. The Applied Biosystems ABI Prism 7900 was used for qRT-PCR. Samples were incubated at 95°C for 15 minutes, followed by 40 cycles at 95°C for 15 seconds and 60°C for 1 minute. In nontemplate control replicates of each gene, no false positives were detected, and all the assays were done in triplicate. Quantitative RT-PCR triplicate runs were repeated on a separate day to confirm reproducibility.

Statistical Analysis

We screened the transcriptome for associations between candidate gene expression and outcomes using linear regression analysis. Categorical variables were compared by Chi-square tests. Overall survival was estimated using the Kaplan-Meier method. Survival curve estimates were compared by the log-rank test. Cox proportional-hazards regression was performed on independent variables that were added sequentially in a stepwise fashion such that they were entered if $P < .05$ and removed if $P > .10$. Statistical calculations were done with MedCalc Version 7.0.1.0 software (Mariakerke, Belgium). Two-sided P values $< .05$ were considered statistically significant. Where applicable, the cutoff point for stratifying gene expression groups was determined using the Maxstat statistical package in R (The R Foundation for Statistical Computing, Version 2.0.0, Vienna, Austria. ISBN 3-900051-00-3, URL: http://cran.r-project.org/).

Results

Candidate Genes Selected from the Screening Microarray

Using a cDNA-based microarray that included 35,518 spots representing 10,671 unique genes, we screened the transcriptome for

Table 1. Sixty-Eight Genes with Increased mRNA Expression in Hepatic Metastases Relative to Primary Colon Tumors from the Same Patient

Locus ID	Symbol	Gene	Spots	N	>1.5×	>2×	>4×	>10×	ON	CLUST
8991	SELENBP1	selenium binding protein 1	1	30	56.7%	43.3%	23.3%	6.7%	0.0%	3
163732	CITED4	Cbp/p300-interacting transactivator, with Glu/Asp-rich carboxy-terminal domain, 4	1	26	53.8%	38.5%	23.1%	7.7%	0.0%	3
4060	LUM	lumican	4	32	62.5%	43.8%	15.6%	0.0%	0.0%	5
5266	PI3	protease inhibitor 3, skin-derived (SKALP)	1	26	53.8%	50.0%	11.5%	3.8%	0.0%	3
27290	SPINK4	serine protease inhibitor, Kazal type 4	1	21	52.4%	28.6%	28.6%	9.5%	0.0%	3
27248	XTP3TPB	XTP3-transactivated protein B	1	26	50.0%	34.6%	19.2%	7.7%	0.0%	3
9518	GDF15	growth differentiation factor 15	2	31	51.6%	38.7%	16.1%	3.2%	0.0%	6
374354	FLJ25621	FLJ25621 protein	1	23	52.2%	34.8%	17.4%	4.3%	0.0%	3
2192	FBLN1	fibulin 1	2	15	53.3%	46.7%	6.7%	0.0%	0.0%	5
11167	FSTL1	follistatin-like 1	2	31	61.3%	41.9%	3.2%	0.0%	0.0%	5
4313	MMP2	matrix metalloproteinase 2 (gelatinase A, 72kDa gelatinase, 72kDa type IV collagenase)	2	26	65.4%	34.6%	3.8%	0.0%	0.0%	5
2049	EPHB3	EphB3	1	27	48.1%	33.3%	18.5%	3.7%	0.0%	6
800	CALD1	caldesmon 1	1	28	50.0%	39.3%	10.7%	3.6%	0.0%	5
57535	KIAA1324	maba1	1	27	51.9%	33.3%	7.4%	3.7%	3.7%	3
4535	MTND1	NADH dehydrogenase 1	2	30	63.3%	36.7%	0.0%	0.0%	0.0%	4
1634	DCN	decorin	6	32	53.1%	28.1%	15.6%	0.0%	0.0%	5
26073	POLDIP2	polymerase (DNA-directed), delta interacting protein 2	1	27	51.9%	29.6%	14.8%	0.0%	0.0%	3
26047	CNTNAP2	contactin associated protein-like 2	1	21	52.4%	28.6%	4.8%	0.0%	9.5%	4
1513	CTSK	cathepsin K (pycnodysostosis)	1	15	53.3%	33.3%	6.7%	0.0%	0.0%	5
131177	FAM3D	family with sequence similarity 3, member D	1	29	48.3%	24.1%	13.8%	6.9%	0.0%	3
5786	PTPRA	protein tyrosine phosphatase, receptor type, A	1	29	58.6%	34.5%	0.0%	0.0%	0.0%	4
5327	PLAT	plasminogen activator, tissue	2	28	60.7%	28.6%	0.0%	0.0%	0.0%	5
10406	WFDC2	WAP four-disulfide core domain 2	2	25	52.0%	24.0%	12.0%	0.0%	0.0%	3
1278	COL1A2	collagen, type I, alpha 2	2	32	43.8%	31.3%	9.4%	3.1%	0.0%	5
132160	FLJ32332	likely ortholog of mouse protein phosphatase 2C eta	1	31	48.4%	32.3%	6.5%	0.0%	0.0%	4
4536	MTND2	NADH dehydrogenase 2	2	31	54.8%	29.0%	3.2%	0.0%	0.0%	4
7433	VIPR1	vasoactive intestinal peptide receptor 1	1	21	57.1%	28.6%	0.0%	0.0%	0.0%	3
4091	MADH6	MAD, mothers against decapentaplegic homolog 6 (Drosophila)	1	28	60.7%	25.0%	0.0%	0.0%	0.0%	4
1277	COL1A1	collagen, type I, alpha 1	1	20	50.0%	30.0%	5.0%	0.0%	0.0%	5
1504	CTRB1	chymotrypsinogen B1	1	30	53.3%	26.7%	3.3%	0.0%	0.0%	4
6741	SSB	Sjogren syndrome antigen B (autoantigen La)	1	27	55.6%	25.9%	0.0%	0.0%	0.0%	4
27122	DKK3	dickkopf homolog 3 (Xenopus laevis)	1	20	50.0%	25.0%	5.0%	0.0%	0.0%	5
23469	PHF3	PHD finger protein 3	1	30	60.0%	20.0%	0.0%	0.0%	0.0%	4
5908	RAP1B	RAP1B, member of RAS oncogene family	1	30	53.3%	26.7%	0.0%	0.0%	0.0%	4
5295	PIK3R1	phosphoinositide-3-kinase, regulatory subunit, polypeptide 1 (p85 alpha)	1	25	52.0%	24.0%	4.0%	0.0%	0.0%	4
3297	HSF1	heat shock transcription factor 1	1	30	56.7%	23.3%	0.0%	0.0%	0.0%	4
2	A2M	alpha-2-macroglobulin	1	30	46.7%	26.7%	6.7%	0.0%	0.0%	5
81558	LOC81558	C/EBP-induced protein	1	29	51.7%	24.1%	3.4%	0.0%	0.0%	4
5801	PTPRR	protein tyrosine phosphatase, receptor type, R	1	29	44.8%	31.0%	3.4%	0.0%	0.0%	3
2487	FRZB	frizzled-related protein	1	18	55.6%	16.7%	5.6%	0.0%	0.0%	3
6348	CCL3	chemokine (C-C motif) ligand 3	1	27	51.9%	22.2%	3.7%	0.0%	0.0%	4
2006	ELN	elastin (supravalvular aortic stenosis, Williams-Beuren syndrome)	1	27	48.1%	29.6%	0.0%	0.0%	0.0%	4
84859	MGC4126	hypothetical protein MGC4126	2	31	45.2%	25.8%	6.5%	0.0%	0.0%	5
4513	MTCO2	cytochrome c oxidase II	3	31	51.6%	22.6%	3.2%	0.0%	0.0%	4
146880	MGC40489	hypothetical protein MGC40489	1	30	46.7%	26.7%	3.3%	0.0%	0.0%	4
83483	PLVAP	plasmalemma vesicle associated protein	1	25	48.0%	28.0%	0.0%	0.0%	0.0%	5
6678	SPARC	secreted protein, acidic, cysteine-rich (osteonectin)	1	29	44.8%	24.1%	6.9%	0.0%	0.0%	5
132241	LOC132241	hypothetical protein LOC132241	1	29	51.7%	20.7%	3.4%	0.0%	0.0%	4
67122	Nrarp	Notch-regulated ankyrin repeat protein	1	28	42.9%	28.6%	3.6%	0.0%	0.0%	3
398	ARHGDIG	Rho GDP dissociation inhibitor (GDI) gamma	1	27	44.4%	18.5%	11.1%	0.0%	0.0%	3
51599	LISCH7	liver-specific bHLH-Zip transcription factor	1	30	50.0%	23.3%	0.0%	0.0%	0.0%	4
81788	SNARK	likely ortholog of rat SNF1/AMP-activated protein kinase	1	29	51.7%	20.7%	0.0%	0.0%	0.0%	4
57605	PITPNM2	phosphatidylinositol transfer protein, membrane-associated 2	1	29	51.7%	20.7%	0.0%	0.0%	0.0%	4
51332	SPTBN5	spectrin, beta, non-erythrocytic 5	1	25	48.0%	20.0%	4.0%	0.0%	0.0%	4
4541	MTND6	NADH dehydrogenase 6	6	32	43.8%	25.0%	3.1%	0.0%	0.0%	4
56940	DUSP22	dual specificity phosphatase 22	1	27	48.1%	22.2%	0.0%	0.0%	0.0%	5
2580	GAK	cyclin G associated kinase	1	27	51.9%	18.5%	0.0%	0.0%	0.0%	4
23432	GPR161	G protein-coupled receptor 161	1	29	48.3%	20.7%	0.0%	0.0%	0.0%	4
583	BBS2	Bardet-Biedl syndrome 2	1	29	48.3%	20.7%	0.0%	0.0%	0.0%	4
2045	EPHA7	EphA7	1	28	46.4%	21.4%	0.0%	0.0%	0.0%	4
3189	HNRPH3	heterogeneous nuclear ribonucleoprotein H3 (2H9)	1	31	48.4%	19.4%	0.0%	0.0%	0.0%	4
1158	CKM	creatine kinase, muscle	1	30	46.7%	20.0%	0.0%	0.0%	0.0%	4
9775	DDX48	DEAD (Asp-Glu-Ala-Asp) box polypeptide 48	1	24	45.8%	20.8%	0.0%	0.0%	0.0%	4
10551	AGR2	anterior gradient 2 homolog (Xenopus laevis)	2	29	41.4%	24.1%	0.0%	0.0%	0.0%	3
1999	ELF3	E74-like factor 3 (ets domain transcription factor, epithelial-specific)	1	30	43.3%	20.0%	0.0%	0.0%	0.0%	3
27336	HTATSF1	HIV TAT specific factor 1	1	29	44.8%	17.2%	0.0%	0.0%	0.0%	4
7125	TNNC2	troponin C2, fast	1	28	42.9%	14.3%	0.0%	0.0%	0.0%	4
3040	HBA2	hemoglobin, alpha 2	1	27	48.1%	3.7%	0.0%	0.0%	0.0%	5

Each gene is identified by its LocusLink ID, symbol, and name. The "Spots" column indicates the number of spots (cDNA clones) used to measure each gene's expression. The "*N*" column shows the maximum number of patient samples where a particular gene was measured; this number was used in calculating the average percent prevalence across patients. The average prevalence, for cuts of 1.5-, 2-, 4-, and 10- fold increased M/T expression, or cases where the gene was only detected in the metastatic tumor sample ("ON"), is shown as a percentage of the patients where the gene was measured. The "CLUST" column indicates which of the clusters shown in Figure 1 each gene belongs to. The genes are ordered by the sum of the prevalence values, in decreasing order.

Table 2. Seventy-Six Genes with Decreased mRNA Expression in Hepatic Metastases Relative to Primary Colon Tumors from the Same Patient

Locus ID	Symbol	Gene	Spots	N	>1.5×	>2×	>4×	>10×	OFF	CLUST
12	SERPINA3	serine (or cysteine) proteinase inhibitor, clade A (alpha-1 antiproteinase, antitrypsin), member 3	2	25	64.0%	60.0%	48.0%	24.0%	0.0%	1
51761	ATP8A2	ATPase, aminophospholipid transporter-like, Class I, type 8A, member 2	1	15	60.0%	53.3%	40.0%	26.7%	0.0%	1
51129	ANGPTL4	angiopoietin-like 4	1	18	66.7%	61.1%	22.2%	5.6%	0.0%	2
348	APOE	apolipoprotein E	2	32	59.4%	50.0%	31.3%	6.3%	0.0%	5
5004	ORM1	orosomucoid 1	1	19	57.9%	42.1%	26.3%	15.8%	0.0%	1
3240	HP	haptoglobin	7	29	51.7%	41.4%	27.6%	17.2%	0.0%	1
6347	CCL2	chemokine (C-C motif) ligand 2	2	21	71.4%	42.9%	14.3%	4.8%	0.0%	5
27295	PDLIM3	PDZ and LIM domain 3	1	14	64.3%	50.0%	7.1%	0.0%	7.1%	5
213	ALB	albumin	1	14	50.0%	35.7%	21.4%	14.3%	0.0%	2
7076	TIMP1	tissue inhibitor of metalloproteinase 1 (erythroid potentiating activity, collagenase inhibitor)	3	31	67.7%	41.9%	6.5%	0.0%	0.0%	6
2335	FN1	fibronectin 1	4	32	56.3%	40.6%	18.8%	0.0%	0.0%	6
710	SERPING1	serine (or cysteine) proteinase inhibitor, clade G (C1 inhibitor), member 1, (angioedema, hereditary)	1	26	50.0%	34.6%	26.9%	3.8%	0.0%	5
8553	BHLHB2	basic helix-loop-helix domain containing, class B, 2	1	26	57.7%	53.8%	0.0%	0.0%	0.0%	6
3303	HSPA1A	heat shock 70kDa protein 1A	4	31	48.4%	35.5%	22.6%	3.2%	0.0%	3
6373	CXCL11	chemokine (C-X-C motif) ligand 11	1	11	63.6%	18.2%	9.1%	0.0%	18.2%	5
56937	TMEPAI	transmembrane, prostate androgen induced RNA	1	25	48.0%	40.0%	16.0%	4.0%	0.0%	6
6035	RNASE1	ribonuclease, RNase A family, 1 (pancreatic)	1	29	55.2%	31.0%	13.8%	6.9%	0.0%	3
2316	FLNA	filamin A, alpha (actin binding protein 280)	2	31	51.6%	41.9%	12.9%	0.0%	0.0%	5
768	CA9	carbonic anhydrase IX	1	18	44.4%	33.3%	16.7%	0.0%	11.1%	4
2885	GRB2	growth factor receptor-bound protein 2	1	21	57.1%	33.3%	14.3%	0.0%	0.0%	5
7564	ZNF16	zinc finger protein 16 (KOX 9)	1	27	51.9%	44.4%	7.4%	0.0%	0.0%	6
4070	TACSTD2	tumor-associated calcium signal transducer 2	1	28	50.0%	28.6%	17.9%	7.1%	0.0%	6
7052	TGM2	transglutaminase 2 (C polypeptide, protein-glutamine-gamma-glutamyltransferase)	1	28	57.1%	32.1%	14.3%	0.0%	0.0%	6
4071	TM4SF1	transmembrane 4 superfamily member 1	1	29	51.7%	41.4%	6.9%	3.4%	0.0%	4
10397	NDRG1	N-myc downstream regulated gene 1	1	30	56.7%	40.0%	6.7%	0.0%	0.0%	2
2207	FCER1G	Fc fragment of IgE, high affinity I, receptor for; gamma polypeptide	1	21	61.9%	33.3%	4.8%	0.0%	0.0%	5
1152	CKB	creatine kinase, brain	3	32	50.0%	31.3%	12.5%	6.3%	0.0%	3
1514	CTSL	cathepsin L	4	31	54.8%	29.0%	9.7%	3.2%	0.0%	5
652	BMP4	bone morphogenetic protein 4	1	24	50.0%	37.5%	8.3%	0.0%	0.0%	6
633	BGN	biglycan	1	24	58.3%	37.5%	0.0%	0.0%	0.0%	1
3936	LCP1	lymphocyte cytosolic protein 1 (L-plastin)	1	23	47.8%	26.1%	13.0%	8.7%	0.0%	5
2878	GPX3	glutathione peroxidase 3 (plasma)	1	18	55.6%	33.3%	5.6%	0.0%	0.0%	1
7422	VEGF	vascular endothelial growth factor	2	30	53.3%	33.3%	6.7%	0.0%	0.0%	6
4256	MGP	matrix Gla protein	1	30	46.7%	36.7%	10.0%	0.0%	0.0%	1
374	AREG	amphiregulin (schwannoma-derived growth factor)	1	29	44.8%	27.6%	13.8%	6.9%	0.0%	4
7701	ZNF142	zinc finger protein 142 (clone pHZ-49)	1	28	46.4%	32.1%	14.3%	0.0%	0.0%	3
51366	DD5	progestin induced protein	1	27	44.4%	37.0%	11.1%	0.0%	0.0%	6
10457	GPNMB	glycoprotein (transmembrane) nmb	1	26	50.0%	30.8%	11.5%	0.0%	0.0%	5
22822	PHLDA1	pleckstrin homology-like domain, family A, member 1	1	24	50.0%	33.3%	8.3%	0.0%	0.0%	6
10123	ARL7	ADP-ribosylation factor-like 7	3	32	46.9%	31.3%	6.3%	6.3%	0.0%	6
4316	MMP7	matrix metalloproteinase 7 (matrilysin, uterine)	6	32	46.9%	31.3%	9.4%	3.1%	0.0%	6
3576	IL8	interleukin 8	1	21	47.6%	33.3%	4.8%	4.8%	0.0%	6
5163	PDK1	pyruvate dehydrogenase kinase, isoenzyme 1	1	29	58.6%	31.0%	0.0%	0.0%	0.0%	2
1649	DDIT3	DNA-damage-inducible transcript 3	1	28	46.4%	35.7%	7.1%	0.0%	0.0%	2
7033	TFF3	trefoil factor 3 (intestinal)	1	27	44.4%	22.2%	14.8%	3.7%	3.7%	3
4493	MT1E	metallothionein 1E (functional)	1	26	46.2%	30.8%	11.5%	0.0%	0.0%	3
7481	WNT11	wingless-type MMTV integration site family, member 11	1	17	52.9%	23.5%	5.9%	0.0%	5.9%	4
10381	TUBB4	tubulin, beta, 4	1	15	60.0%	26.7%	0.0%	0.0%	0.0%	1
5270	SERPINE2	serine (or cysteine) proteinase inhibitor, clade E (nexin, plasminogen activator inhibitor type 1), member 2	1	28	46.4%	32.1%	3.6%	3.6%	0.0%	6
9590	AKAP12	A kinase (PRKA) anchor protein (gravin) 12	1	20	50.0%	25.0%	5.0%	5.0%	0.0%	2
54206	*MIG-6*	mitogen-inducible gene 6	1	31	45.2%	35.5%	3.2%	0.0%	0.0%	2
11067	C10orf10	chromosome 10 open reading frame 10	1	24	62.5%	20.8%	0.0%	0.0%	0.0%	6
2159	F10	coagulation factor X	1	18	50.0%	33.3%	0.0%	0.0%	0.0%	4
57561	ARRDC3	arrestin domain containing 3	3	27	59.3%	22.2%	0.0%	0.0%	0.0%	6
4495	MT1G	metallothionein 1G	1	27	44.4%	22.2%	11.1%	3.7%	0.0%	3
10628	TXNIP	thioredoxin interacting protein	5	32	46.9%	31.3%	3.1%	0.0%	0.0%	3
3939	LDHA	lactate dehydrogenase A	2	32	53.1%	25.0%	3.1%	0.0%	0.0%	6
6890	TAP1	transporter 1, ATP-binding cassette, sub-family B (MDR/TAP)	1	24	45.8%	20.8%	8.3%	4.2%	0.0%	3
1942	EFNA1	ephrin-A1	1	28	46.4%	32.1%	0.0%	0.0%	0.0%	4
136	ADORA2B	adenosine A2b receptor	1	22	50.0%	27.3%	0.0%	0.0%	0.0%	3
11145	HRASLS3	HRAS-like suppressor 3	1	26	46.2%	30.8%	0.0%	0.0%	0.0%	6
84951	CTEN	C-terminal tensin-like	1	21	52.4%	19.0%	4.8%	0.0%	0.0%	6
90637	LOC90637	hypothetical protein LOC90637	1	29	44.8%	27.6%	3.4%	0.0%	0.0%	2
7045	TGFBI	transforming growth factor, beta-induced, 68kDa	1	24	50.0%	25.0%	0.0%	0.0%	0.0%	6
5230	PGK1	phosphoglycerate kinase 1	1	32	46.9%	25.0%	3.1%	0.0%	0.0%	6
64065	PERP	PERP, TP53 apoptosis effector	1	28	46.4%	17.9%	3.6%	3.6%	0.0%	6
9531	BAG3	BCL2-associated athanogene 3	1	28	42.9%	25.0%	3.6%	0.0%	0.0%	6
23023	KIAA0779	KIAA0779 protein	1	21	47.6%	23.8%	0.0%	0.0%	0.0%	3
567	B2M	beta-2-microglobulin	1	28	46.4%	17.9%	0.0%	0.0%	0.0%	3
2317	FLNB	filamin B, beta (actin binding protein 278)	1	28	42.9%	14.3%	7.1%	0.0%	0.0%	3
665	BNIP3L	BCL2/adenovirus E1B 19kDa interacting protein 3-like	2	30	46.7%	16.7%	0.0%	0.0%	0.0%	2
7431	VIM	vimentin	1	28	42.9%	14.3%	3.6%	0.0%	0.0%	5
91452	ACBD5	acyl-Coenzyme A binding domain containing 5	1	27	44.4%	14.8%	0.0%	0.0%	0.0%	4
1508	CTSB	cathepsin B	1	31	48.4%	9.7%	0.0%	0.0%	0.0%	6

Table 2.   (*continued*)

Locus ID	Symbol	Gene	Spots	N	>1.5×	>2×	>4×	>10×	OFF	CLUST
55818	JMJD1	jumonji domain containing 1	1	28	42.9%	14.3%	0.0%	0.0%	0.0%	6
5763	PTMS	parathymosin	1	31	41.9%	12.9%	0.0%	0.0%	0.0%	3

The columns are the same as in Table 1, except that the prevalence columns indicate percentage of patients exhibiting downregulation and the "OFF" column indicates the percentage of patients where expression was detected in the primary tumor but not the metastasis.

genes that were differentially expressed in unresected metastases of colorectal cancer relative to their primary tumors in 42 patients. The characteristics of these patients were: median age 59 years (range 31-82); 61% male, 29% female; primary tumor site 43% right colon, 33% left colon, 2% right and left colon, 22% rectum; primary node status 15% positive, 85% negative; time to progression 91% </= 12 months (synchronous) and 9% >12 months (metachronous); the median number of hepatic metastases was 3 with a range of 1-11; and the average CEA was 141.

In the screen, 22,344 spots representing 8,027 unique genes met criteria for analysis. From the 10,671 genes in the microarray, 144 demonstrated differential expression between primary colon tumors and matched hepatic metastases. Differential expression was defined as at least 1.5-fold difference in at least 20% of matched primary and metastatic samples. Transcripts showing a tendency for increased expression in the metastases relative to primary tumors are in Table 1, while those exhibiting decreased expression are in Table 2. Hierarchical clustering applying the Pearson correlation for the distance metric and complete linkage identified six distinct spot clusters, which are shown in the heat map of differentially expressed genes (Figure 1).

We found 68 genes that were consistently up-regulated and 76 that were down-regulated in CRCLM relative to matched primary tumors.

From this group of 144 differentially expressed genes, 7 were selected for validation based on the association between mRNA level (using values obtained from the microarray) and clinical outcome (Table 3): lumican, a proteoglycan of the extracellular matrix reported to be overexpressed in colorectal breast, neuroendocrine, and other cancers [21]; tissue inhibitor of metalloproteinase 1 (TIMP1), an inhibitor of matrix metalloproteinases and modulator of other diverse processes in cancer cells [22]; basic helix-loop-helix domain containing B2 (BHLHB2), a transcription factor that is induced by hypoxia within tumors [23]; fibronectin, an abundant extracellular matrix protein that contributes to altered stromal remodeling during tumorigenesis [24]; TM4SF1 (transmembrane 4 superfamily member 1), a tumor-associated antigen that regulates cancer cell motility and invasion [25]; serpine2, an extracellular serine protease that is overexpressed in pancreatic, colon, and stomach cancers that may facilitate invasive processes [26]; and *MIG-6*, a putative tumor suppressor that negatively regulates the ErbB family of receptor tyrosine kinases [27,28].

Association of Candidate Genes in CRC Metastases with Clinical Outcome

To determine whether the expression of the candidate genes identified above as correlating with clinical outcome for unresectable patients with colorectal metastases confined to the liver also applied to
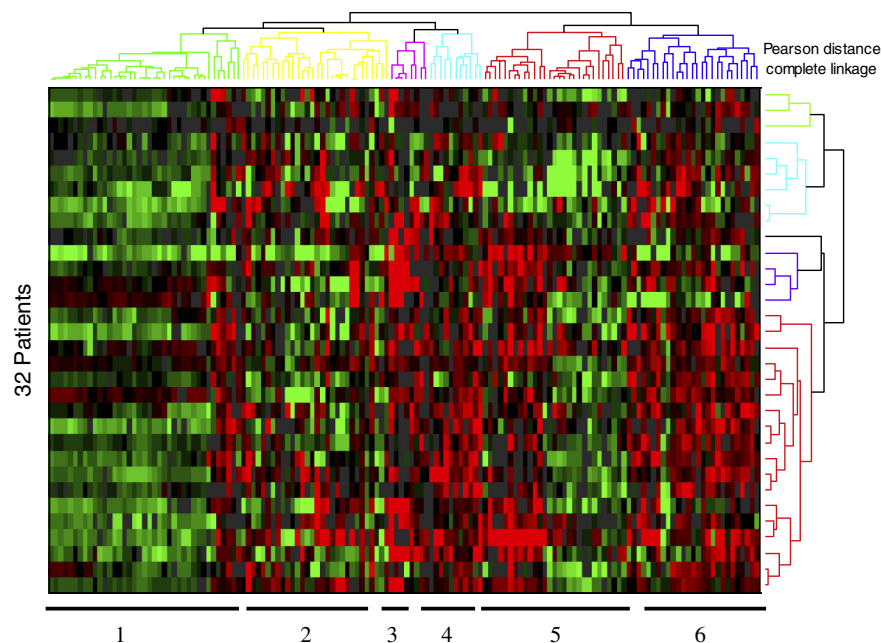

Figure 1. Expression of genes that show significant up- or downregulation in metastatic tumors of the liver relative to primary colon tumors from the same patient in 20% or more of the patient population with 99% certainty based on a sampling of 32 patients. Upregulation is indicated by shades of red, downregulation is indicated by shades of green, black indicates no change, and gray indicates ratios that failed to pass detection or consistency criteria. Tables 1 and 2 indicate which cluster each of the genes belongs to.

Table 3. Seven Candidate Genes Were Selected on the Basis of Differential Expression Between Colorectal Liver Metastases and Their Corresponding Primary Tumor and an Association Between mRNA Level (as Determined by the Microarray Analysis) and Clinical Outcome (*P*<.05)

Candidate Gene	Name	Relative Expression in CRCLM	Clinical Variable
LUM	Lumican	Higher	OS
TIMP1	Tissue inhibitor of metalloproteinase 1	Lower	TTP TS
BHLHB2	Basic helix-loop-helix domain containing, class B, 2	Lower	OS
FN1	Fibronectin	Lower	TTP
TM4SF1	Transmembrane 4 superfamily member 1	Lower	OS
MIG-6	Mitogen-inducible gene 6	Lower	TTP
SER2	Serpine2	Lower	OS TS

OS, overall survival; *TTP*, time to progression of liver metastases.

patients undergoing potentially curative hepatectomy for CRCLM, we performed qRT-PCR of the 7 candidate genes on CRCLM from 56 additional patients. qRT-PCR allowed us to more accurately quantify the levels of each transcript than obtaining such information from an array and therefore allowed more accurate substratification of patients into *MIG-6*–high and *MIG-6*–low groups. Since we often did not have matching primary tumors for these patients, mRNA levels of the metastasis and normal tissue were compared. The baseline clinical variables and their association with overall survival of the group of 56 patients who underwent potentially curative

hepatectomy are in Table 4. The median follow-up time of the surviving patients in this group was 97 months after hepatectomy (range 55-107 months).

To determine if expression of any of the seven genes was associated with survival after hepatectomy, we dichotomized patients into high- and low-expression groups according to the median relative mRNA level. In this analysis, *MIG-6* was the only gene whose expression was predictive of survival (Table 5). Patients in the lower 50th percentile of *MIG-6* expression had a median survival that was over twice as long as that of patients in the upper 50th percentile (*P* = .01, Table 5). Using Maxstat software to optimize the cutoff value for high and low *MIG-6* expression, a statistically significant difference in overall survival was found by Kaplan-Meier analysis (log-rank *P* = .0024, Figure 2). This approach also showed that none of the candidate genes, including *MIG-6*, was predictive of liver disease–free survival (LDFS) (Table 5).

High- and Low-CRS Patients Further Stratified by MIG-6 Gene Expression

Because *MIG-6* was the only gene whose expression predicted survival, we were interested in whether patients with a high or low CRS could be further stratified by *MIG-6* expression. This led us to perform qRT-PCR of *MIG-6* mRNA on 25 additional patients with CRCLM (total *n* = 81 patients). To determine if the CRS predicted survival after hepatectomy in this cohort, we generated Kaplan-Meier survival estimates of low CRS (0-2) and high CRS (3-5). Although

Table 4. Results of Univariate Association of Clinicopathologic Variables with Overall Survival

Variable	n	Median Survival (Months)	Hazard Ratio	95% CI	P Value
Age					
<60	26	68	0.63	0.33-1.18	.15
≥60	30	36			
Sex					
Female	18	37	0.88	0.46-1.70	.71
Male	38	32			
Date of hepatectomy					
After January 1, 2000	19	29	1.28	0.65-2.71	.44
Before January 1, 2000	37	40			
Primary tumor site					
Colon	47	36	1.03	0.46-2.34	.94
Rectum	9	51			
Disease-free interval					
Metachronous	23	54	0.61	0.33-1.17	.14
Synchronous	33	33			
Hepatic lobe involvement					
Unilobar	40	36	1.32	0.66-2.58	.44
Bilobar	16	36			
Primary tumor node status					
N0	14	43	0.84	0.42-1.69	.63
N1	41	36			
Preoperative CEA					
<200 ng/ml	39	33	1.37	0.52-3.44	.55
≥200 ng/ml	6	65			
Diameter of largest met					
<5.0 cm	28	58	0.50	0.25-0.91	.03
≥5.0 cm	28	30			
Number of metastases					
Solitary	27	54	0.57	0.30-1.05	.07
Multiple	29	29			
Hepatectomy EBL					
<1000 ml	30	36	1.16	0.62-2.19	.64
≥1000 ml	25	33			
Hepatectomy margin					
<1.0 cm	27	40	1.11	0.59-2.08	.74
≥1.0 cm	29	31			

Preoperative CEA level was not obtained in 13 patients. Primary tumor nodal status was unknown in two patients. *CEA*, carcinoembryonic antigen; *met*, metastasis.

Table 5. Univariate Analysis of Candidate Genes

Candidate Gene Expression	n	Median Survival (mos)	Hazard Ratio (95% CI)	P Value Survival	Median LDFS (mos)	Hazard Ratio (95% CI)	P Value LDFS
LUM							
Low	28	50	0.64	.19	51	0.55	.10
High	27	32	(0.30-1.28)		20	(0.24-1.14)	
TIMP1							
Low	28	57	0.60	.14	51	0.51	.07
High	28	31	(0.29-1.19)		20	(0.23-1.06)	
BHLHB2							
Low	28	57	0.59	.13	NR	0.55	.11
High	28	31	(0.28-1.17)		27	(0.26-1.16)	
FN1							
Low	28	57	0.63	.18	46	0.80	.54
High	28	31	(0.30-1.26)		27	(0.37-1.69)	
TM4SF1							
Low	28	42	0.90	.77	46	0.94	.86
High	28	31	(0.44-1.83)		27	(0.44-1.99)	
Mig-6							
Low	28	67	0.42	**.01**	NR	0.55	.10
High	28	29	(0.18-0.80)		20	(0.24-1.12)	
SER2							
Low	28	42	0.79	.50	46	0.76	.47
High	27	31	(0.38-1.61)		20	(0.35-1.62)	

Quantitative RT-PCR was performed on colorectal liver metastases from 56 additional patients that underwent hepatectomy. Patients above and below the median expression level were compared by log-rank testing.

the median survival of the low CRS group was not reached, the median survival of the high-CRS group was 25 months. The Kaplan-Meier survival estimates for the low-CRS group were higher than those for the high-CRS group (log-rank P = .005, Figure 3). Within the low-CRS group (n = 40), stratifying by median *MIG-6* expression resulted in low– (n = 20) and high– (n = 20) *MIG-6* expression subgroups (Figure 4A). Median survival was 33 months for patients in the subgroup with low CRS and high *MIG-6* but was not reached in

the subgroup with low CRS and low *MIG-6*. When patients in the low-CRS group were substratified by the median *MIG-6* level, statistically distinct survival curves by log-rank testing (P = .03) resulted.

When patients in the high-CRS group (n = 41) were stratified by median *MIG-6* expression, the median survival was almost twice as long in the low–*MIG-6* subgroup (n = 21) as it was in the high–*MIG-6* subgroup (n =20) (Figure 4B). As with the low-CRS group, patients with a high CRS could be effectively substratified by median *MIG-6* expression, resulting in statistically distinct survival curves by log-rank testing (P = .04).
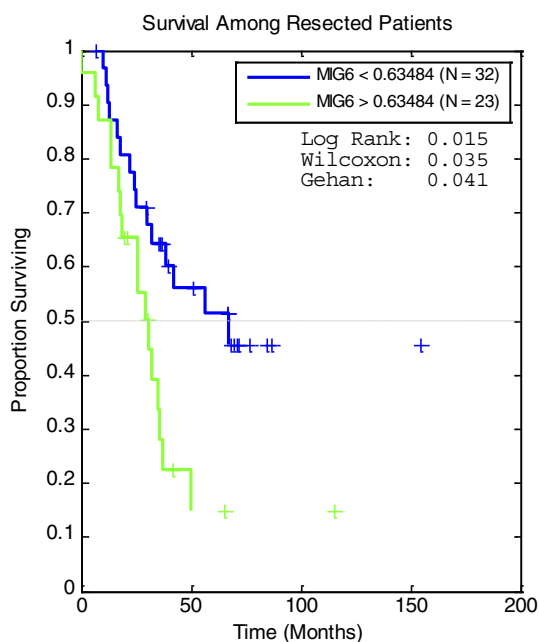

Figure 2. Kaplan-Meier survival estimates of survival in patients after resection stratified by *MIG-6* expression. MaxStat software was used to optimize the cutoff value for high and low *MIG-6* expression. A statistically significant difference in overall survival was found by this analysis (log-rank P = .0024)
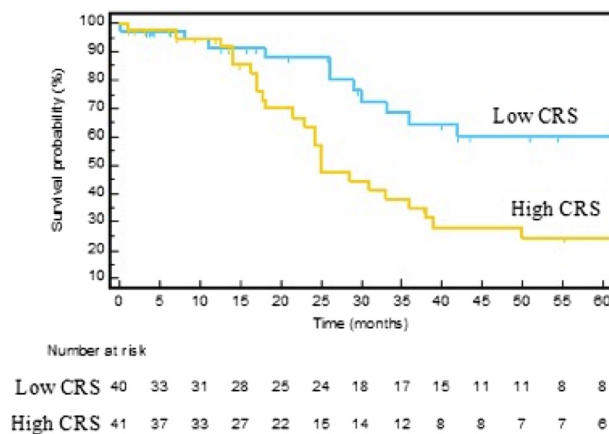

Figure 3. Patient stratification for overall survival by CRS. Kaplan-Meier survival estimates comparing low-CRS (0-2) vs. high-CRS (3–5) groups. The median overall survival was 25 months in the high-CRS group, but it was not reached in the low-CRS group (P = .005). Fourteen patients did not have preoperative CEA levels and were excluded from the analysis. Numbers below the figure are life tables designating how many patients are represented in the survival curves.
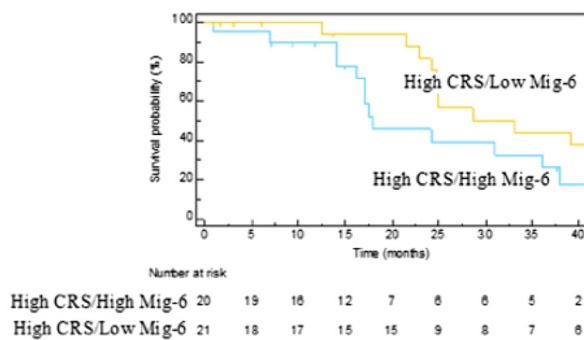
A
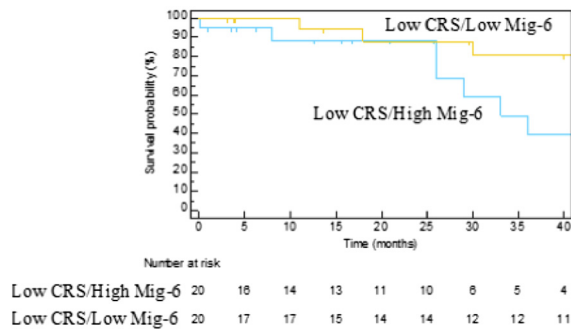
B

Figure 4. *MIG-6* can substratify patients beyond the CRS. Patients divided into low-CRS (0-2) and high-CRS (3-5) groups were further stratified by median *MIG-6* expression. **(A)** Within the low-CRS group, patients were separated into two groups: those in the upper 50th percentile of *MIG-6* expression and those in the lower 50th percentile. The median overall survival was 33 months in the upper–*MIG-6* subgroup and was not reached in the lower–*MIG-6* group (*P* = .03). **(B)** Similarly, within the high-CRS group, patients were separated into two groups: those in the upper 50th percentile of *MIG-6* expression and those in the lower 50th percentile. The median overall survival in the upper– and lower–*MIG-6* subgroups was 18 and 33 months, respectively (*P* = .04). Numbers below the figure are life tables designating how many patients are represented in the survival curves.

Discussion

We used gene expression profiling to identify differentially expressed genes in CRCLM relative to matched primary tumors. Among the genes identified, *MIG-6* (also called gene-33, RALT, or ERRFI1) encodes an adaptor protein that interacts with and inhibits the activities of members of the ErbB receptor family and other receptor tyrosine kinases [29,30]. The human *MIG-6* gene is on chromosome 1p36, a locus associated with many cancers [31], and *MIG-6* is proposed to be a tumor suppressor [28,32]. Consistent with this, *MIG-6* expression is reduced in human breast, skin, pancreatic, and ovarian cancers, and diminished *MIG-6* expression in patients with breast cancer correlates with poor survival [33,34]. Furthermore, germline disruption of the murine *MIG-6* gene leads to cancers of the lung, gallbladder, bile duct, skin, and gastrointestinal tract [29,32]. Identification of *MIG-6* as a gene that has low expression in CRCLM relative to matched primary cancers may suggest that *MIG-6* can act as a suppressor of metastasis.

We found that elevated *MIG-6* mRNA expression was associated with decreased survival after hepatectomy of CRCLM. This observation should be considered in concert with results showing that *MIG-6* has diverse functions in both physiology and pathology which, depending on context, can promote survival or cell death.

MIG-6 transcription is induced by diverse stimuli including growth factors [35,36], hormones [37], cytokines [29,38], and hypoxia [39]. *MIG-6* is a feedback inhibitor of all members of the ErbB receptor family [29,30], with the EGFR being best investigated. Activation of the EGFR increases *MIG-6* transcription in a RAS-ERK–dependent fashion [40,41], leading to accumulation of the *MIG-6* protein within 60-90 minutes. In turn, *MIG-6* binds the tyrosine kinase domain of the activated EGFR, inactivates the receptor tyrosine kinase, and thereby attenuates EGFR action. Thus, *MIG-6* $^{-/-}$ mice display epidermal hyperplasia and have an increased susceptibility to skin carcinogenesis, which is caused by unabated EGFR signaling [29]. During lung development and vascularization, the absence of *MIG-6* leads to hyperplasia of several tissues, as well as to enhanced apoptosis of endothelial cells and diminished expression of angiogenic factors [42]. Considered together, the observations summarized above show that that *MIG-6* may coordinate life and death decision making to facilitate tissue homeostasis [27,28].

It has been commonly assumed that *MIG-6* functions solely as a tumor suppressor and that EGFR acts in an oncogenic manner. However, several studies have established the ability of EGFR to induce apoptosis in breast cancer cells [43–47], while others have established the ability of *MIG-6* to protect human breast cancer cells from apoptosis [42,48]. A strong basis exists for believing that unbalanced expression of *MIG-6* relative to the EGFR activates internalized EGFR, where it may initiate apoptosis [43,44,46,47,49]. Recent studies show that phosphorylation of *MIG-6* may negatively affect its interaction with the EGFR as well as its capacity to induce trafficking of the EGFR [30,50,51]. Since the activity of *MIG-6* on EGFR is dependent on its phosphorylation status, localization, and protein levels, it may be necessary to interrogate these attributes of *MIG-6* in patients to know its true prognostic significance.

Petroda et al. [52] recently showed that the identification of molecular subtypes of colorectal metastases across individual patients can complement clinical risk stratification to distinguish low-, intermediate-, and high-risk patients with distinct 10-year survivals. The present study builds on this approach by showing that CRCLM patients could be stratified within their respective CRS group by relative *MIG-6* expression to improve prognostic accuracy for patients. Our observations should encourage evaluation of patient outcomes when *MIG-6* expression and *MIG-6* expression relative to EGFR localization and abundance are considered in a larger, prospective study.

This study had several limitations. The patients whose tumor specimens were used in the screening array had unresected CRCLM, whereas patients in the validation group underwent hepatectomy. Ideally, screening and validation groups have identical clinical features and undergo identical treatment. Furthermore, the samples utilized were not randomly selected but rather represented patients who had tissue available for research. We defined high and low *MIG-6* expression by retrospectively selecting the most significant cutoff by log-rank testing. We also used the median expression of *MIG-6* to dichotomize patients as a relatively unbiased means of stratifying beyond the CRS. We acknowledge that reaching conclusions using cut points from maximally selected statistics and multiple hypothesis

testing requires further validation. The ultimate confirmation of the association between *MIG-6* expression and survival after hepatectomy requires larger and perhaps prospective studies.

Despite these limitations, many of which are inevitable in research with human tumor specimens, we believe that our central conclusions are of interest: high *MIG-6* expression is a negative prognostic feature in CRCLM; furthermore, determination of *MIG-6* expression can augment the accuracy of prognostic schemes that rely on clinico-pathologic data.

Author Contributions

D. B. D., D. T. R., and R. S. W. planned the studies. D. T. R., R. J. A., R. S. W., and D. B. D. wrote the manuscript. K. T., E. K. B., E. K. N., M. H. L., and R. J. A. prepared the figures and tables and contributed to data analysis.

References

[1] Abdalla EK, Vauthey JN, Ellis LM, Ellis V, Pollock R, Broglio KR, Hess K, and Curley SA (2004). Recurrence and outcomes following hepatic resection, radiofrequency ablation, and combined resection/ablation for colorectal liver metastases. *Ann Surg* **239**, 818–825 [discussion 825-817].

[2] Portier G, Elias D, Bouche O, Rougier P, Bosset JF, Saric J, Belghiti J, Piedbois P, Guimbaud R, and Nordlinger B, et al (2006). Multicenter randomized trial of adjuvant fluorouracil and folinic acid compared with surgery alone after resection of colorectal liver metastases: FFCD ACHBTH AURC 9002 trial. *J Clin Oncol* **24**, 4976–4982.

[3] Goldberg RM, Sargent DJ, Morton RF, Fuchs CS, Ramanathan RK, Williamson SK, Findlay BP, Pitot HC, and Alberts SR (2004). A randomized controlled trial of fluorouracil plus leucovorin, irinotecan, and oxaliplatin combinations in patients with previously untreated metastatic colorectal cancer. *J Clin Oncol* **22**, 23–30.

[4] Tournigand C, Andre T, Achille E, Lledo G, Flesh M, Mery-Mignard D, Quinaux E, Couteau C, Buyse M, and Ganem G, et al (2004). FOLFIRI followed by FOLFOX6 or the reverse sequence in advanced colorectal cancer: a randomized GERCOR study. *J Clin Oncol* **22**, 229–237.

[5] Fong Y, Fortner J, Sun RL, Brennan MF, and Blumgart LH (1999). Clinical score for predicting recurrence after hepatic resection for metastatic colorectal cancer: analysis of 1001 consecutive cases. *Ann Surg* **230**, 309–318 [discussion 318-321].

[6] Konopke R, Kersting S, Distler M, Dietrich J, Gastmeier J, Heller A, Kulisch E, and Saeger HD (2009). Prognostic factors and evaluation of a clinical score for predicting survival after resection of colorectal liver metastases. *Liver Int* **29**, 89–102.

[7] Nagashima I, Takada T, Nagawa H, Muto T, and Okinaga K (2006). Proposal of a new and simple staging system of colorectal liver metastasis. *World J Gastroenterol* **12**, 6961–6965.

[8] Nordlinger B, Guiguet M, Vaillant JC, Balladur P, Boudjema K, Bachellier P, and Jaeck D (1996). Surgical resection of colorectal carcinoma metastases to the liver. A prognostic scoring system to improve case selection, based on 1568 patients. Association Francaise de Chirurgie. *Cancer* **77**, 1254–1262.

[9] Rees M, Tekkis PP, Welsh FK, O'Rourke T, and John TG (2008). Evaluation of long-term survival after hepatic resection for metastatic colorectal cancer: a multifactorial model of 929 patients. *Ann Surg* **247**, 125–135.

[10] Vauthey JN, Pawlik TM, Ribero D, Wu TT, Zorzi D, Hoff PM, Xiong HQ, Eng C, Lauwers GY, and Mino-Kenudson M, et al (2006). Chemotherapy regimen predicts steatohepatitis and an increase in 90-day mortality after surgery for hepatic colorectal metastases. *J Clin Oncol* **24**, 2065–2072.

[11] Tanaka K, Adam R, Shimada H, Azoulay D, Levi F, and Bismuth H (2003). Role of neoadjuvant chemotherapy in the treatment of multiple colorectal metastases to the liver. *Br J Surg* **90**, 963–969.

[12] Adam R, Pascal G, Castaing D, Azoulay D, Delvart V, Paule B, Levi F, and Bismuth H (2004). Tumor progression while on chemotherapy: a contraindication to liver resection for multiple colorectal metastases?*Ann Surg* **240**, 1052–1061 [discussion 1061-1054].

[13] Kemeny N (2007). Presurgical chemotherapy in patients being considered for liver resection. *Oncologist* **12**, 825–839.

[14] Arru M, Aldrighetti L, Castoldi R, Di Palo S, Orsenigo E, Stella M, Pulitano C, Gavazzi F, Ferla G, and Di Carlo V, et al (2008). Analysis of prognostic factors

[15] influencing long-term survival after hepatic resection for metastatic colorectal cancer. *World J Surg* **32**, 93–103.

[15] Tomlinson JS, Jarnagin WR, DeMatteo RP, Fong Y, Kornprat P, Gonen M, Kemeny N, Brennan MF, Blumgart LH, and D'Angelica M (2007). Actual 10-year survival after resection of colorectal liver metastases defines cure. *J Clin Oncol* **25**, 4575–4580.

[16] Zakaria S, Donohue JH, Que FG, Farnell MB, Schleck CD, Ilstrup DM, and Nagorney DM (2007). Hepatic resection for colorectal metastases: value for risk scoring systems? *Ann Surg* **246**, 183–191.

[17] Dupre A, Rehman A, Jones RP, Parker A, Diaz-Nieto R, Fenwick SW, Poston GJ, and Malik HZ (2018). Validation of clinical prognostic scores for patients treated with curative-intent for recurrent colorectal liver metastases. *J Surg Oncol* **117**, 1330–1336.

[18] Sinicrope FA, Okamoto K, Kasi PM, and Kawakami H (2016). Molecular biomarkers in the personalized treatment of colorectal cancer. *Clin Gastroenterol Hepatol* **14**, 651–658.

[19] Wang E, Miller LD, Ohnmacht GA, Liu ET, and Marincola FM (2000). High-fidelity mRNA amplification for gene profiling. *Nat Biotechnol* **18**, 457–459.

[20] Grifantini R, Bartolini E, Muzzi A, Draghi M, Frigimelica E, Berger J, Ratti G, Petracca R, Galli G, and Agnusdei M, et al (2002). Previously unrecognized vaccine candidates against group B meningococcus identified by DNA microarrays. *Nat Biotechnol* **20**, 914–921.

[21] Ishiwata T, Cho K, Kawahara K, Yamamoto T, Fujiwara Y, Uchida E, Tajiri T, and Naito Z (2007). Role of lumican in cancer cells and adjacent stromal tissues in human pancreatic cancer. *Oncol Rep* **18**, 537–543.

[22] Jackson HW, Defamie V, Waterhouse P, and Khokha R (2017). TIMPs: versatile extracellular regulators in cancer. *Nat Rev Cancer* **17**, 38–53.

[23] Wang W, Reiser-Erkan C, Michalski CW, Raggi MC, Quan L, Yupei Z, Friess H, Erkan M, and Kleeff J (2010). Hypoxia inducible BHLHB2 is a novel and independent prognostic marker in pancreatic ductal adenocarcinoma. *Biochem Biophys Res Commun* **401**, 422–428.

[24] Wang K, Seo BR, Fischbach C, and Gourdon D (2016). Fibronectin mechanobiology regulates tumorigenesis. *Cell Mol Bioeng* **9**, 1–11.

[25] Cao J, Yang JC, Ramachandran V, Arumugam T, Deng DF, Li ZS, Xu LM, and Logsdon CD (2016). TM4SF1 regulates pancreatic cancer migration and invasion in vitro and in vivo. *Cell Physiol Biochem* **39**, 740–750.

[26] Neesse A, Wagner M, Ellenrieder V, Bachem M, Gress TM, and Buchholz M (2007). Pancreatic stellate cells potentiate proinvasive effects of SERPINE2 expression in pancreatic cancer xenograft tumors. *Pancreatology* **7**, 380–385.

[27] Anastasi S, Lamberti D, Alema S, and Segatto O (2016). Regulation of the ErbB network by the *MIG-6* feedback loop in physiology, tumor suppression and responses to oncogene-targeted therapeutics. *Semin Cell Dev Biol* **50**, 115–124.

[28] Zhang YW and Vande Woude GF (2007). *MIG-6*, signal transduction, stress response and cancer. *Cell Cycle* **6**, 507–513.

[29] Ferby I, Reschke M, Kudlacek O, Knyazev P, Pante G, Amann K, Sommergruber W, Kraut N, Ullrich A, and Fassler R, et al (2006). *MIG-6* is a negative regulator of EGF receptor-mediated skin morphogenesis and tumor formation. *Nat Med* **12**, 568–573.

[30] Park E, Kim N, Ficarro SB, Zhang Y, Lee BI, Cho A, Kim K, Park AKJ, Park WY, and Murray B, et al (2015). Structure and mechanism of activity-based inhibition of the EGF receptor by *MIG-6*. *Nat Struct Mol Biol* **22**, 703–711.

[31] Henrich KO, Schwab M, and Westermann F (2012). 1p36 tumor suppression— a matter of dosage? *Cancer Res* **72**, 6079–6088.

[32] Zhang YW, Staal B, Su Y, Swiatek P, Zhao P, Cao B, Resau J, Sigler R, Bronson R, and Vande Woude GF (2007). Evidence that *MIG-6* is a tumor-suppressor gene. *Oncogene* **26**, 269–276.

[33] Amatschek S, Koenig U, Auer H, Steinlein P, Pacher M, Gruenfelder A, Dekan G, Vogl S, Kubista E, and Heider KH, et al (2004). Tissue-wide expression profiling using cDNA subtraction and microarrays to identify tumor-specific genes. *Cancer Res* **64**, 844–856.

[34] Anastasi S, Sala G, Huiping C, Caprini E, Russo G, Iacovelli S, Lucini F, Ingvarsson S, and Segatto O (2005). Loss of RALT/*MIG-6* expression in ERBB2-amplified breast carcinomas enhances ErbB-2 oncogenic potency and favors resistance to herceptin. *Oncogene* **24**, 4540–4548.

[35] Anastasi S, Fiorentino L, Fiorini M, Fraioli R, Sala G, Castellani L, Alema S, Alimandi M, and Segatto O (2003). Feedback inhibition by RALT controls signal output by the ErbB network. *Oncogene* **22**, 4221–4234.

[36] Fiorentino L, Pertica C, Fiorini M, Talora C, Crescenzi M, Castellani L, Alema S, Benedetti P, and Segatto O (2000). Inhibition of ErbB-2 mitogenic and

transforming activity by RALT, a mitogen-induced signal transducer which binds to the ErbB-2 kinase domain. *Mol Cell Biol* **20**, 7735–7750.

[37] Jeong JW, Lee HS, Lee KY, White LD, Broaddus RR, Zhang YW, Vande Woude GF, Giudice LC, Young SL, and Lessey BA, et al (2009). *MIG-6* modulates uterine steroid hormone responsiveness and exhibits altered expression in endometrial disease. *Proc Natl Acad Sci U S A* **106**, 8677–8682.

[38] Zhang YW, Su Y, Lanning N, Swiatek PJ, Bronson RT, Sigler R, Martin RW, and Vande Woude GF (2005). Targeted disruption of *MIG-6* in the mouse genome leads to early onset degenerative joint disease. *Proc Natl Acad Sci U S A* **102**, 11740–11745.

[39] Endo H, Okami J, Okuyama H, Nishizawa Y, Imamura F, and Inoue M (2017). The induction of *MIG-6* under hypoxic conditions is critical for dormancy in primary cultured lung cancer cells with activating EGFR mutations. *Oncogene* **36**, 2824–2834.

[40] Fiorini M, Ballaro C, Sala G, Falcone G, Alema S, and Segatto O (2002). Expression of RALT, a feedback inhibitor of ErbB receptors, is subjected to an integrated transcriptional and post-translational control. *Oncogene* **21**, 6530–6539.

[41] Hackel PO, Gishizky M, and Ullrich A (2001). *MIG-6* is a negative regulator of the epidermal growth factor receptor signal. *Biol Chem* **382**, 1649–1662.

[42] Jin N, Cho SN, Raso MG, Wistuba I, Smith Y, Yang Y, Kurie JM, Yen R, Evans CM, and Ludwig T, et al (2009). *MIG-6* is required for appropriate lung development and to ensure normal adult lung homeostasis. *Development* **136**, 3347–3356.

[43] Ettenberg SA, Rubinstein YR, Banerjee P, Nau MM, Keane MM, and Lipkowitz S (1999). cbl-b inhibits EGF-receptor-induced apoptosis by enhancing ubiquitination and degradation of activated receptors. *Mol Cell Biol Res Commun* **2**, 111–118.

[44] Hyatt DC and Ceresa BP (2008). Cellular localization of the activated EGFR determines its effect on cell growth in MDA-MB-468 cells. *Exp Cell Res* **314**, 3415–3425.

[45] Reinehr R and Haussinger D (2012). CD95 death receptor and epidermal growth factor receptor (EGFR) in liver cell apoptosis and regeneration. *Arch Biochem Biophys* **518**, 2–7.

[46] Rush JS, Quinalty LM, Engelman L, Sherry DM, and Ceresa BP (2012). Endosomal accumulation of the activated epidermal growth factor receptor (EGFR) induces apoptosis. *J Biol Chem* **287**, 712–722.

[47] Wendt MK, Williams WK, Pascuzzi PE, Balanis NG, Schiemann BJ, Carlin CR, and Schiemann WP (2015). The antitumorigenic function of EGFR in metastatic breast cancer is regulated by expression of *MIG-6*. *Neoplasia* **17**, 124–133.

[48] Xu J, Keeton AB, Wu L, Franklin JL, Cao X, and Messina JL (2005). Gene 33 inhibits apoptosis of breast cancer cells and increases poly(ADP-ribose) polymerase expression. *Breast Cancer Res Treat* **91**, 207–215.

[49] Chang X, Izumchenko E, Solis LM, Kim MS, Chatterjee A, Ling S, Monitto CL, Harari PM, Hidalgo M, and Goodman SN, et al (2013). The relative expression of *MIG-6* and EGFR is associated with resistance to EGFR kinase inhibitors. *PLoS One* **8**e68966.

[50] Boopathy GTK, Lynn JLS, Wee S, Gunaratne J, and Hong W (2018). Phosphorylation of *MIG-6* negatively regulates the ubiquitination and degradation of EGFR mutants in lung adenocarcinoma cell lines. *Cell Signal* **43**, 21–31.

[51] Wang Z, Raines LL, Hooy RM, Roberson H, Leahy DJ, and Cole PA (2013). Tyrosine phosphorylation of *MIG-6* reduces its inhibition of the epidermal growth factor receptor. *ACS Chem Biol* **8**, 2372–2376.

[52] Pitroda SP, Khodarev NN, Huang L, Uppal A, Wightman SC, Ganai S, Joseph N, Pitt J, Brown M, and Forde M, et al (2018). Integrated molecular subtyping defines a curable oligometastatic state in colorectal liver metastasis. *Nat Commun* **9**, 1793.